

## Researching and Development of an Autonomous Underwater Vehicles with Capability of Collecting Solar Energy

Nguyen Van Tuan<sup>1,2\*</sup>, Dinh Van Phong<sup>1</sup>, Nguyen Chi Hung<sup>1</sup>

<sup>1</sup> Hanoi University of Science and Technology, Hanoi, Vietnam

<sup>2</sup> Phenikaa University, Yen Nghia, Ha Dong, Hanoi, Viet Nam

\*Email: tuan.nguyenvan@phenikaa-uni.edu.vn

### Abstract

*Autonomous Underwater Vehicles (AUV) is an unmanned underwater device with capability of performing a variety of missions in the water environment such as ocean operation, offshore waters, polluted water investigation including: marine scientific research, maritime monitoring, exploration, marine economics, oil and gas, security and defense, surveillance and measurement and in rescue and salve. In this article, the authors developed a model of AUV with retractable wings and evaluate the efficiency of solar energy collection. The establishment of the controller to adapt the stability requirements, in accordance with the model of equipment S-AUV (Solar - Autonomous Underwater Vehicles) was built. The hydrodynamic equations with the predefined conditions were modeled and solved. The Hierarchical Sliding Mode Controller (HSMC) for the S-AUV were applied in this research. Experimental results showed that the efficiency of the collection of the solar cell has been significantly improved comparing to a diving equipment without retractable energy wings. In addition, the simulation results showed that the developed controller performed much better control quality, adhering to the set value with the error within the permissible limit.*

Keywords: Autonomous underwater vehicles, energy solar, underactuated system, control AUV, hierarchical sliding mode controller.

### 1. Introduction

Autonomous Underwater Vehicles (AUV) have been used in many industrial applications such as oceanography, fisheries, environmental monitoring, security and defense, rescue and salve, etc. With the automatic operation function, AUV is very suitable for missions required for exploring deep water/ocean [1]. The AUV is an automatic, programmable device that is self-propelled, or remotely controlled by sending commands from the monitoring center or semi-automatic operation without the need for an operator depending on the targeted function. The AUV plays an important role such as in marine exploitation, oil and gas installation and large-scale subsea surveys, offshore research, etc .

The ability to store energy on AUV is an important factor in the design and operation of the AUV. With the limitations of size, mass and different design requirements, the energy storage on the AUV is often limited, so the operation time of the AUV is limited. The integration of AUV and energy replenishment systems have been studied for decades [2]. The IMTP Institute of Technology and the Russian Academy of Sciences have evaluated the technologies required for a solar-powered AUV [2]. One of the products of this development program is the manufacture and testing of an Autonomous

Underwater Vehicles with capability of collecting solar energy namely SAUV I [2].

Vietnam is a country with a coastline of over 3,000 km and a large territorial sea with many islands. Therefore, the study of AUV will have a lot of potential applications in economic activities, society, security and defense and in scientific research. Moreover, as a subtropical tropical country, Vietnam has a huge amount of solar radiation with hours of sunshine from 1,400 to 2,600 hours/year. The North has an average of 1,400 - 2,100 hours of sunshine per year, the South from Da Nang City on average from 2,000 to 2,600 hours of sunshine per year. The observed data shows that the average radiation energy across the country per day is from 3.3 to 5.7 kWh/m<sup>2</sup> [3]. The potential for energy use in almost every region of the country is very promising.

With the ability to move automatically in the water environment, AUV is very suitable for missions that explore deep, toxic or need long-term activities. However, the fixed energy wing increases the motion resistance on the AUV under the water [5], since the design structure of the diving equipment affects drag when moving. The greater the drag force is, the energy loss increases. The relationship between drag force and the shape, size, and velocity of the AUV diving equipment is represented by the following formula:

$$F_{drag} = \frac{1}{2} \cdot \rho \cdot u^2 \cdot C_d \cdot S \quad (1)$$

where  $F_{drag}$  is the resistance acting on the AUV in the direction of movement,  $\rho$  is the density of water,  $u$  is the velocity of the AUV,  $C_d$  is the form resistance coefficient and  $S$  is the projected area of the AUV on the plane perpendicular to the direction of motion.

The linear controllers have been used for controllers for AUV by many researchers [5, 6]. PID controller is mainly applied to linear systems, however there are also some PID extending controllers to nonlinear systems that can be adopted for AUV [7]. The controllers for AUV are Sliding Mode Controls [8], adaptive controllers [9], Fuzzy logic controllers [10], Model Predictive Controller (MPC) [11], controllers based on neural networks [12] and Object-oriented control method. In this paper, the author focuses on the Sliding Mode Controller for a small S-AUV with added solar energy. The outstanding advantage of the Hierarchical Sliding Mode Controller is its stability and robustness even in the case of system with noise or when the object's parameters change over time.

The authors designed and built a small AUV with energy supplementation by retractable solar wings. The energy wings remain closing in moving states, and starting opening when the AUV approaches the surface of the energy-harvesting water radiated by sunlight in the day time. Optimizing the energy collected by the wings to reduce the size and shape of the S-AUV, which can be changed when moving, will have several benefits including (i) reducing the drag impact on the S-AUV, (ii) increasing solar energy collection efficiency, (iii) reducing energy consumption and (iv) supporting the S-AUV to operate for a long time without recharging steps.

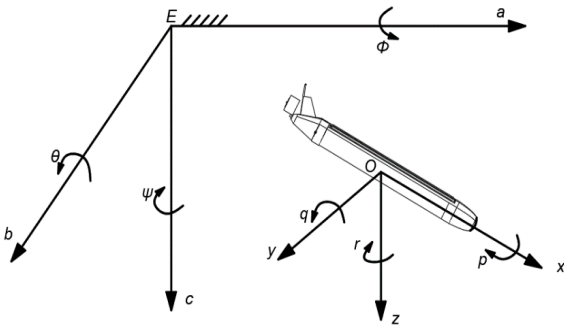


Fig. 1. The dynamic coordinate system  $xyz$  and fixed coordinate system  $abc$

## 2. Dynamics of S-AUV Model

### 2.1. Coordinates

The dynamic model of the S-AUV is built on the basis of mechanical theory, the principles of kinetics and statics. Hydrodynamic models of the S-AUV are used to design control systems for the S-AUV that

meet specific objectives such as motion trajectory control, dive depth control, direction control, ... In general, the movement of S-AUV can be represented by equations of motion with six degrees of freedom (6-DOF) [5]. Parameters such as the direction of motion, force and torque, speed and position for the S-AUV are shown in Table. 1 and Fig. 1.

Table 1. Parameter symbols are represented in dynamic and fixed coordinate systems

DOF	Motion	Forces and moments	Velocity	Position and Euler angles
1	Surge ( $x$ -direction)	$X$	$u$	$x$
2	Sway ( $y$ -direction)	$Y$	$v$	$y$
3	Heave ( $z$ -direction)	$Z$	$w$	$z$
4	Roll (Rotation about $x$ )	$K$	$p$	$\phi$
5	Pitch (Rotation about $y$ )	$M$	$q$	$\theta$
6	Yaw (Rotation about $z$ )	$N$	$r$	$\psi$

Velocity vector  $v$ , reference vector  $\eta$  can be represented as follows:

$$\begin{cases} \eta = [\eta_1^T, \eta_2^T]^T \in R^6 \\ v = [v_1^T, v_2^T]^T \in R^6 \end{cases} \quad (2)$$

where:

$$\begin{cases} \eta_1^* = [x, y, z]^T \in R^3 \\ \eta_2^* = [\phi, \theta, \psi]^T \in R^3 \end{cases} \text{ and } \begin{cases} v_1 = [u, v, w]^T \in R^3 \\ v_2 = [p, q, r]^T \in R^3 \end{cases}$$

The first-order derivative of the position vector is related to the velocity vector through the below transformation:

$$\begin{cases} \dot{\eta}_1^* = J_1(\eta_2^*)v_1 \\ \dot{\eta}_2^* = J_2(\eta_2^*)v_2 \end{cases} \quad (3)$$

Combining (2) and (3) creates equations that describe the position and direction of S-AUV:

$$\begin{bmatrix} \dot{\eta}_1^* \\ \dot{\eta}_2^* \end{bmatrix} = \begin{bmatrix} J_1(\eta_2^*) & 0_{3 \times 3} \\ 0_{3 \times 3} & J_2(\eta_2^*) \end{bmatrix} \begin{bmatrix} v_1 \\ v_2 \end{bmatrix} \Leftrightarrow \dot{\eta} = J(\eta)v \quad (4)$$

with:

$$J_1(\eta_2^*) = \begin{bmatrix} c(\theta) \cdot c(\psi) & J_{12} & J_{13} \\ c(\theta) \cdot s(\psi) & J_{22} & J_{23} \\ -s(\theta) & s(\phi) \cdot c(\theta) & c(\phi) \cdot c(\theta) \end{bmatrix}$$

with:  $c=\cos; s=\sin$

$$J_{12} = s(\phi).s(\theta).c(\psi) - c(\phi).s(\psi)$$

$$J_{13} = c(\phi).s(\theta).c(\psi) + s(\phi).s(\psi)$$

$$J_{22} = s(\phi).s(\theta).s(\psi) + c(\phi).c(\psi)$$

$$J_{23} = c(\phi).s(\theta).s(\psi) - s(\phi).c(\psi)$$

$$J_2(\eta_{2*}) = \begin{bmatrix} 1 & s(\phi)\tan(\theta) & cs(\phi)\tan(\theta) \\ 0 & c(\phi) & -s(\phi) \\ 0 & s(\phi)\sec(\theta) & c(\phi)\sec(\theta) \end{bmatrix}$$

## 2.2. Dynamics with 4 Degrees of Freedom

To simplify the small types of AUV we can remove 2 unnecessary degrees of freedom: angle  $\theta$  (pitch) and angle  $\phi$  (roll). Hence the equations of movement of the S-AUV 4 degrees of freedom are expressed through the quantities (propulsion, a steering wing, two auxiliary rudders combined with a pump system for floating diving). Coordinate position  $(x, y)$ , direction of S-AUV ( $\psi$ - yaw) and position on axis  $z$  (diving depth).

In this study, the authors focus on constructing the hierarchical sliding mode controller with the S-AUV's parameter model which is appropriately calculated and selected. Four degrees of freedom movement model of S-AUV include following:  $\eta = [x, y, z, \psi]^T$  is the position vector of the device in axes  $Ox, Oy, Oz$  and the directional angle of the S-AUV rotates around the axis  $Oz$ ;  $v = [u, v, w, r]^T$  is a vector of long velocity in the directions  $Ox, Oy, Oz$  and the rotational velocity around axis  $Oz$ .

The general dynamic equation for a S-AUV with 4 degrees of freedom is as follows:

$$\begin{cases} \dot{\eta} = J(\eta)v \\ M\dot{v} + C(v)v + D(v)v = \tau^* \end{cases} \quad (5)$$

where:

$$M = \begin{bmatrix} m + X_{\dot{u}} & 0 & X_{\dot{w}} & -my_g \\ 0 & m + Y_{\dot{v}} & 0 & Y_{\dot{r}} + mx_g \\ Z_{\dot{u}} & 0 & m + Z_{\dot{w}} & 0 \\ -my_g & mx_g + N_{\dot{v}} & 0 & I_z + N_{\dot{r}} \end{bmatrix},$$

$$J(\eta) = \begin{bmatrix} \cos(\psi) & -\sin(\psi) & 0 & 0 \\ \sin(\psi) & \cos(\psi) & 0 & 0 \\ 0 & 0 & 1 & 0 \\ 0 & 0 & 0 & 1 \end{bmatrix},$$

$$C = \begin{bmatrix} 0 & -mr & 0 & -mx_g r - a_2 \\ mr & 0 & 0 & -my_g r + a_1 \\ 0 & 0 & 0 & 0 \\ mx_g r + a_2 & my_g r - a_1 & 0 & 0 \end{bmatrix},$$

$$D(v) = \begin{bmatrix} D_{11} & 0 & 0 & 0 \\ 0 & D_{22} & 0 & 0 \\ Z_0 |u| & 0 & D_{33} & 0 \\ 0 & 0 & 0 & D_{44} \end{bmatrix}$$

with:

$$D_{11} = X_u + X_{u|u}|u|$$

$$D_{22} = Y_v + Y_{v|v}|v|$$

$$D_{33} = Z_w + Z_{w|w}|w|$$

$$D_{44} = K_p + K_{p|p}|p|$$

In this case the S-AUV is an underactuated system, consisting of 2 input signals and 4 output signals. Therefore, we separate the mathematical model into two parts, including the underactuated and full actuated system. Position vector  $\eta$  will be separated into 2 parts  $\eta = [\eta_1 \ \eta_2]^T$  and  $\eta_1 = [x \ y]^T$  for a state of full actuated and  $\eta_2 = [z \ \psi]^T$  for a state of underactuated. Similarly, velocity vector  $v$  is divided into two parts with  $v = [v_1 \ v_2]^T$ . The diving gear dynamic equation was rewritten as follows:

$$\begin{cases} \dot{\eta}_1 = J_{11}v_1 + J_{12}v_2 \\ \dot{\eta}_2 = J_{21}v_1 + J_{22}v_2 \\ M_{11}\dot{v}_1 + (C_{11} + D_{11})v_1 + M_{12}\dot{v}_2 + (C_{12} + D_{12})v_2 = \tau \\ M_{21}\dot{v}_1 + (C_{21} + D_{21})v_1 + M_{22}\dot{v}_2 + (C_{22} + D_{22})v_2 = 0 \end{cases} \quad (6)$$

with:

$$M_{11} = \begin{bmatrix} m + X_{\dot{u}} & 0 \\ 0 & m + Y_{\dot{v}} \end{bmatrix}; \quad M_{12} = \begin{bmatrix} X_{\dot{w}} & -my_g \\ 0 & Y_{\dot{r}} + mx_g \end{bmatrix};$$

$$M_{21} = \begin{bmatrix} Z_{\dot{u}} & 0 \\ -my_g & mx_g + N_{\dot{v}} \end{bmatrix}; \quad M_{22} = \begin{bmatrix} m + Z_{\dot{w}} & 0 \\ 0 & I_z + N_{\dot{r}} \end{bmatrix}$$

$$C_{11}(v) = \begin{bmatrix} 0 & -mr \\ mr & 0 \end{bmatrix}; \quad C_{12}(v) = \begin{bmatrix} 0 & -mx_g r - a_2 \\ 0 & -my_g r + a_1 \end{bmatrix};$$

$$C_{21}(v) = \begin{bmatrix} 0 & 0 \\ mx_g r + a_2 & my_g r - a_1 \end{bmatrix}; \quad C_{22}(v) = \begin{bmatrix} 0 & 0 \\ 0 & 0 \end{bmatrix};$$

$$J_{11}(v) = \begin{bmatrix} \cos(\psi) & -\sin(\psi) \\ \sin(\psi) & \cos(\psi) \end{bmatrix}; \quad J_{12}(v) = \begin{bmatrix} 0 & 0 \\ 0 & 0 \end{bmatrix};$$

$$J_{21}(v) = \begin{bmatrix} 0 & 0 \\ 0 & 0 \end{bmatrix}; J_{22}(v) = \begin{bmatrix} 1 & 0 \\ 0 & 1 \end{bmatrix};$$

$$D_{11}(v) = \begin{bmatrix} X_u + X_{|u|}|u| & 0 \\ 0 & Y_v + Y_{|v|}|v| \end{bmatrix};$$

$$D_{12}(v) = \begin{bmatrix} 0 & 0 \\ 0 & 0 \end{bmatrix};$$

$$D_{21}(v) = \begin{bmatrix} Z_w & 0 \\ 0 & 0 \end{bmatrix};$$

$$D_{22}(v) = \begin{bmatrix} Z_w + Z_{|w|}|w| & 0 \\ 0 & K_p + K_{|p|}|p| \end{bmatrix};$$

$$\tau = [\tau_1, \tau_2, 0, 0]$$

$$a_1 = X_u u + X_w w + X_q q$$

$$a_2 = Y_v v + Y_p p + Y_r r$$

Since  $M_{22}$  is the positive definite matrix so from the fourth equation in (6), we have:

$$\dot{v}_2 = -M_{22}^{-1} [M_{21} \dot{v}_1 + (C_{21} + D_{21})v_1 + (C_{22} + D_{22})v_2] \quad (7)$$

Replace (7) into the third equation in (6):

$$\begin{aligned} & M_{11} \dot{v}_1 + (C_{11} + D_{11})v_1 \\ & - M_{12} M_{22}^{-1} [M_{21} \dot{v}_1 + (C_{21} + D_{21})v_1 + (C_{22} + D_{22})v_2] \\ & + (C_{12} + D_{12})v_2 = \tau \end{aligned} \quad (8)$$

Simplify equation (8) we get:

$$\bar{M} \dot{v}_1 + \bar{C}_1 v_1 + \bar{C}_2 v_2 = \tau \quad (9)$$

with:

$$\bar{M} = M_{11} - M_{12} M_{22}^{-1} M_{21}$$

$$\bar{C}_1 = (C_{11} + D_{11}) - M_{12} M_{22}^{-1} (C_{21} + D_{21})$$

$$\bar{C}_2 = (C_{12} + D_{12}) - M_{12} M_{22}^{-1} (C_{22} + D_{22})$$

With the assumption that we can choose the parameters for assuring that the  $\bar{M}$  is positive definite matrix, from the equation (9), we have:

$$\dot{v}_1 = \bar{M}^{-1} (-\bar{C}_1 v_1 - \bar{C}_2 v_2) + \bar{M}^{-1} \tau \quad (10)$$

Replace (10) into the equation (7):

$$\begin{aligned} \dot{v}_2 &= -M_{22}^{-1} [M_{21} \bar{M}^{-1} (\tau - \bar{C}_1 v_1 - \bar{C}_2 v_2) \\ & \quad + (C_{21} + D_{21})v_1 + (C_{22} + D_{22})v_2] \\ \dot{v}_2 &= -M_{22}^{-1} [M_{21} \bar{M}^{-1} (-\bar{C}_1 v_1 - \bar{C}_2 v_2) \\ & \quad + (C_{21} + D_{21})v_1 + (C_{22} + D_{22})v_2] \\ \Leftrightarrow & \quad -M_{22}^{-1} M_{21} \bar{M}^{-1} \tau \end{aligned} \quad (11)$$

Replace (10) and (11) into the system of equations (6), we have the system of dynamic equations of S-AUV as follows:

$$\begin{cases} \dot{\eta}_1 = J_{11} v_1 \\ \dot{v}_1 = \bar{M}^{-1} (-\bar{C}_1 v_1 - \bar{C}_2 v_2) + \bar{M}^{-1} \tau \\ \dot{\eta}_2 = J_{22} v_2 \\ \dot{v}_2 = f(v) \end{cases} \quad (12)$$

with

$$\begin{aligned} f(v) &= -M_{22}^{-1} [M_{21} \bar{M}^{-1} (-\bar{C}_1 v_1 - \bar{C}_2 v_2) \\ & \quad + (C_{21} + D_{21})v_1 + (C_{22} + D_{22})v_2 \\ & \quad - M_{22}^{-1} M_{21} \bar{M}^{-1} \tau \end{aligned}$$

$$\text{where: } J_{12}(v) = \begin{bmatrix} 0 & 0 \\ 0 & 0 \end{bmatrix}; J_{21}(v) = \begin{bmatrix} 0 & 0 \\ 0 & 0 \end{bmatrix}$$

To solve the above problem, the paper proposes to use HSMC controller because this is the most suitable method to control underactuated systems. Therefore, the algorithm structure is used to ensure the stability of the system while still sticking to the given value as shown in Fig. 2.

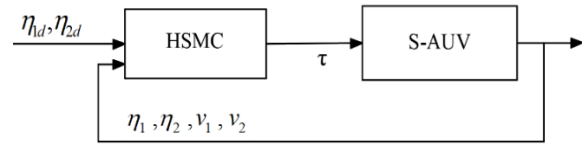


Fig. 2. HSMC controller structure block diagram

From the system of equations (12), we rewrite the generalized form as follows:

$$\begin{cases} \dot{\eta}_1 = J_{11} v_1 \\ \dot{v}_1 = f_1(X) + G_1(X) \tau \\ \dot{\eta}_2 = J_{22} v_2 \\ \dot{v}_2 = f_2(X) + G_2(X) \tau \end{cases} \quad (13)$$

with:

$$X = [\eta_1 \quad v_1 \quad \eta_2 \quad v_2]^T$$

$$f_1(X) = \bar{M}^{-1} (-\bar{C}_1 v_1 - \bar{C}_2 v_2)$$

$$G_1(X) = \bar{M}^{-1}$$

$$\begin{aligned} f_2(X) &= -M_{22}^{-1} [M_{21} \bar{M}^{-1} (-\bar{C}_1 v_1 - \bar{C}_2 v_2) \\ & \quad + (C_{21} + D_{21})v_1 + (C_{22} + D_{22})v_2] \end{aligned}$$

$$G_2(X) = -M_{22}^{-1} M_{21} \bar{M}^{-1}$$

The definition of the error vector between the output signal and the set signal is:

$$e(t) = \begin{bmatrix} e_1 \\ e_2 \\ e_3 \\ e_4 \end{bmatrix} = \begin{bmatrix} \eta_1 - \eta_{1d} \\ v_1 \\ \eta_2 - \eta_{2d} \\ v_2 \end{bmatrix} \quad (14)$$

The definition of the sliding surface is as follows:

$$\begin{cases} s_1 = k_1 e_1 + e_2, (k_1 > 0) \\ s_2 = k_2 e_3 + e_4, (k_2 > 0) \\ S = \lambda s_1 + \beta s_2, (\lambda, \beta > 0) \end{cases} \quad (15)$$

According to the control method HSMC for underactuated system, the controller signal is divided into two components:

$$\tau_n = \tau_{eqn} + \tau_{swn} \quad (16)$$

where:

+  $\tau_{eqn}$  is the signal that is used to control the subsystem in the controller structure Hierarchical Sliding Mode Controller.

+  $\tau_{swn}$  is the signal that is used to control the switching of the system sliding surface.

Consider the first subsystem model:

$$\begin{cases} \dot{\eta}_1 = J_{11} v_1 \\ \dot{v}_1 = f_1(X) + G_1(X)\tau \end{cases} \quad (17)$$

Applying equation (16), we have the control signal for the first and second subsystem as follows:

$$\begin{cases} \tau_1 = \tau_{eq1} + \tau_{sw1} \\ \tau_2 = \tau_{eq2} + \tau_{sw2} \end{cases} \quad (18)$$

The sliding surface derivative  $S_1$  with respect to time we get:

$$\begin{aligned} \dot{s}_1 &= k_1 \dot{e}_1 + \dot{e}_2 = k_1 \dot{e}_1 + f_1(X) + G_1(X)\tau_1 \\ &= k_1 \dot{e}_1 + f_1(X) + G_1(X)(\tau_{eq1} + \tau_{sw1}) \\ &= k_1 \dot{e}_1 + f_1(X) + G_1(X)\tau_{eq1} - a s_1 - b \text{sign}(s_1) \\ &\quad + a s_1 + b \text{sign}(s_1) + G_1(X)\tau_{sw1} \end{aligned} \quad (19)$$

We choose the control signal for the first subsystem as follows:

$$\begin{cases} \tau_{eq1} = -(G_1^{-1}(X))(k_1 J_{11} v_1 + f_1(X)) \\ \tau_{sw1} = -(G_1^{-1}(X))(a s_1 + b \text{sign}(s_1)) \end{cases} \quad (20)$$

Substituting the system of equations (20) into equation (19) we have:

$$\dot{s}_1 = -a s_1 - b \text{sign}(s_1) \quad (21)$$

The control signal for the system consists of two subsystems:

$$\tau = \tau_1 + \tau_2 \quad (22)$$

Select the sliding surface for the first and second subsystems as follows:

$$S = \lambda s_1 + \beta s_2 \quad (23)$$

To ensure stability for the S-AUV, consider Lyapunov function for the closed system as follows:

$$V = \frac{1}{2} S^T \dot{S} \quad (24)$$

Taking derivative  $V$  over time, we get:

$$\frac{\partial V}{\partial t} = S^T \dot{S} \quad (25)$$

From (13), (14), (15) and (25) we have below equation:

$$\begin{aligned} \frac{\partial V}{\partial t} &= S^T \dot{S} \\ &= S^T \cdot [\lambda \dot{s}_1 + \beta \dot{s}_2] \\ &= S^T \cdot \left[ \begin{array}{l} \lambda(k_1 J_{11} v_1 + f_1(X) + G_1(X)\tau - k_1 \dot{\eta}_{1d}) \\ + \beta(k_2 J_{22} v_2 + f_2(X) + G_2(X)\tau - k_2 \dot{\eta}_{2d}) \end{array} \right] \end{aligned}$$

Since  $\eta_{1d}, \eta_{2d}$  are constant values so:  $\dot{\eta}_{1d} = \dot{\eta}_{2d} = 0$ .

Hence:

$$\begin{aligned} \frac{\partial V}{\partial t} &= S^T \dot{S} \\ &= S^T \cdot \left[ \begin{array}{l} \lambda(k_1 J_{11} v_1 + f_1(X) + G_1(X)\tau) \\ + \beta(k_2 J_{22} v_2 + f_2(X) + G_2(X)\tau) \end{array} \right] \\ &= S^T \cdot \left[ \begin{array}{l} \lambda(k_1 J_{11} v_1 + f_1(X) + \\ G_1(X)(\tau_{eq1} + \tau_{sw1} + \tau_{eq2} + \tau_{sw2})) \\ + \beta(k_2 J_{22} v_2 + f_2(X) + \\ G_2(X)(\tau_{eq1} + \tau_{sw1} + \tau_{eq2} + \tau_{sw2})) \end{array} \right] \\ &= S^T \cdot \left[ \begin{array}{l} \lambda(k_1 J_{11} v_1 + f_1(X) + G_1(X)\tau_{eq1}) \\ + \beta(k_2 J_{22} v_2 + f_2(X) + G_2(X)\tau_{eq2}) \\ + \tau_{sw1}(\lambda G_1(X) + \beta G_2(X)) \\ + \tau_{sw2}(\lambda G_1(X) + \beta G_2(X)) \\ + \lambda G_1(X)\tau_{eq2} + \beta G_2(X)\tau_{eq1} \\ + k \cdot S + \delta \text{sgn}(S) - (k \cdot S + \delta \text{sgn}(S)) \end{array} \right] \quad (26) \end{aligned}$$

To ensure the stability of the system through the principle of stability of Lyapunov so that  $\partial V / \partial t$  is negative definite, we choose the following control signals:

$$\begin{cases} \tau_{eq1} = -G_1^{-1}(X)(k_1 J_{11} v_1 + f_1(X)) \\ \tau_{eq2} = -G_2^{-1}(X)(k_2 J_{22} v_2 + f_2(X)) \\ \tau_{sw2} = -(\lambda G_1(X) + \beta G_2(X))^{-1}(\lambda G_1(X)\tau_{eq2} \\ + \beta G_2(X)\tau_{eq1}) - (\lambda G_1(X) \\ + \beta G_2(X))^{-1}(k \cdot S + \delta \text{sgn}(S)) - \tau_{sw1} \end{cases} \quad (27)$$

With values corresponding to (27) and  $s_1 = k_1 e_1 + e_2, s_2 = k_2 e_3 + e_4$  and through the Lyapunov function choose the values for  $e_1 \rightarrow 0; e_2 \rightarrow 0; e_3 \rightarrow 0; e_4 \rightarrow 0$ . Then we get  $s_1 \rightarrow 0, s_2 \rightarrow 0$ .

Replacing (27) into equation (26) we have:

$$\frac{\partial V}{\partial t} = S^T \cdot \dot{S} = -(k \cdot S^T S + \delta S^T \text{sgn}(S)) \leq 0$$

This suggests that the system stability is guaranteed.

Control signals are determined by the following formula:

$$\begin{aligned} \tau &= \tau_{eq1} + \tau_{sw1} + \tau_{eq2} + \tau_{sw2} \\ &= -(G_1^{-1}(X)) \cdot (k_1 J_{11} v_1 + f_1(X)) \\ &\quad - (G_2^{-1}(X)) \cdot (k_2 J_{22} v_2 + f_2(X)) \\ &\quad - (\lambda G_1(X) + \beta g_2(X))^{-1} \\ &\quad \times (\lambda G_1(X) \tau_{eq2} + \beta G_2(X) \tau_{eq1} + k \cdot S + \delta \text{sgn}(S)) \end{aligned} \quad (28)$$

### 3. Simulation and Experimental Results

#### 3.1. Performance of the Collection Solar Energy Test

The S-AUV has been tested to collect solar energy at some localities such as Hai Phong City, Quang Ninh Province (Ha Long Bay) and Hanoi City, as shown in Fig. 5. S-AUV in case of closing and opening as shown in Fig. 3, Fig. 4.

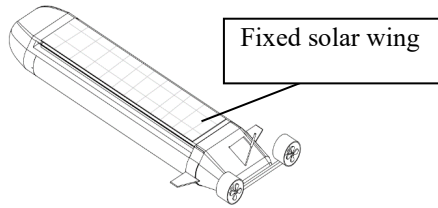


Fig. 3. S-AUV in closed solar wing case

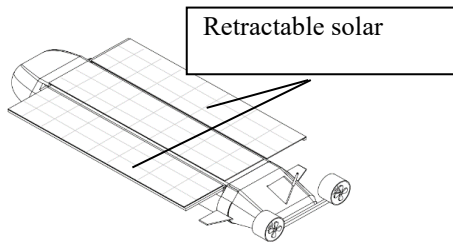


Fig. 4. S-AUV in opened solar wing case



Fig. 5. Testing in Quang Ninh Province

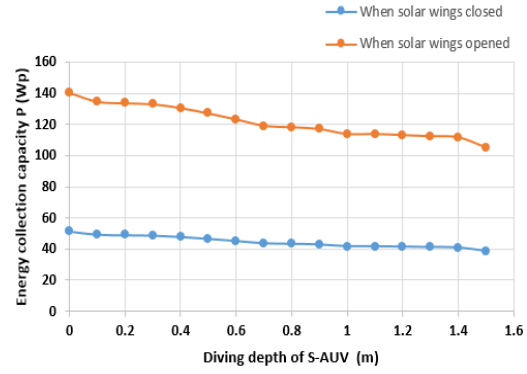


Fig. 6. Solar energy collection chart with solar wing closed and opened at Hai Phong City (2020 Aug)

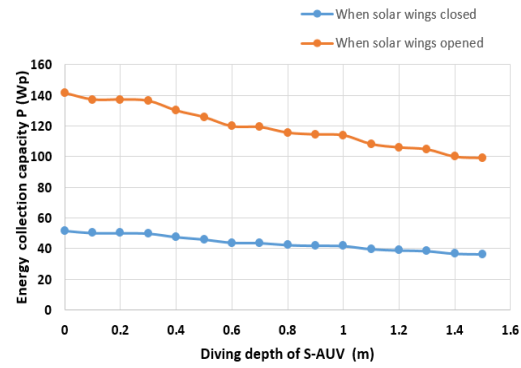


Fig. 7. Solar energy collection chart with solar wing closed and opened at Quang Ninh City (2020 Aug)

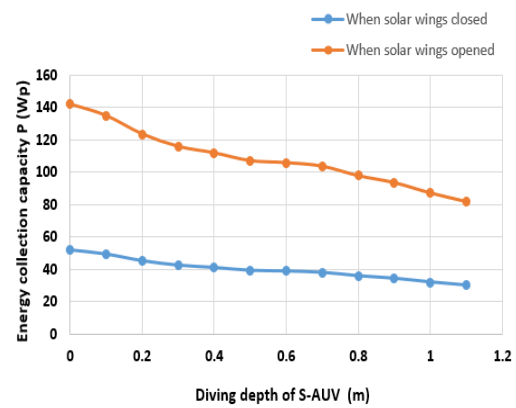


Fig. 8. Solar energy collection chart with solar wing closed and opened at Ha Noi City (2020 Aug)

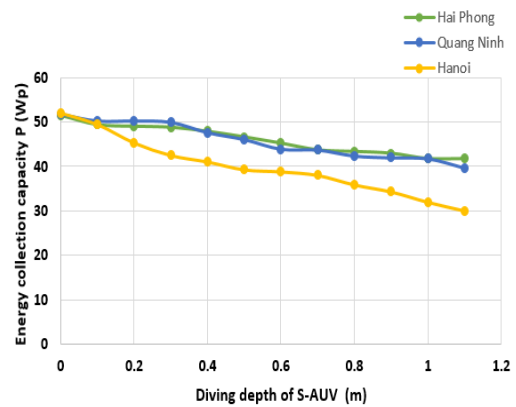


Fig. 9. Solar energy collection with solar wing closed at Hai Phong, Quang Ninh, Hanoi (2020 Aug)

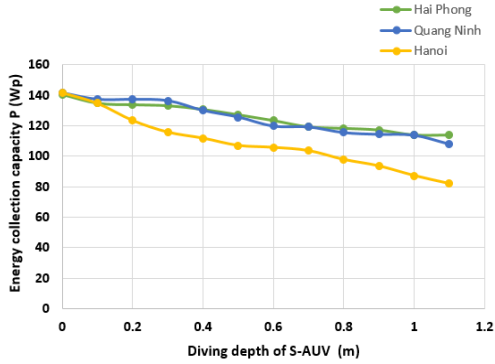


Fig. 10. Solar energy collection with solar wing opened at Hai Phong, Quang Ninh, Hanoi (2020 Aug)

Test conditions: The S-AUV's solar capture capacity measurement was made in the period from 12:00 to 13:00, to avoid the influence of the angle of sunlight. Time to measure sunny days without clouds in August 2020. The average of total radiation in August measured in Quang Ninh Province, Hai Phong City was 17.56 -17.82 MJ/m<sup>2</sup>/day; in Hanoi City is 18.23 MJ/m<sup>2</sup>/day [3].

Fig. 6 , Fig. 7, Fig. 8, Fig. 9, Fig. 10 show that when S-AUV increases the depth of diving, the solar collecting capacity of S-AUV in both fields when opening and closing the energy wing decreases linearly. Opening the retractable energy wing, the solar collector capacity increases, the largest increase is 2.7 times.

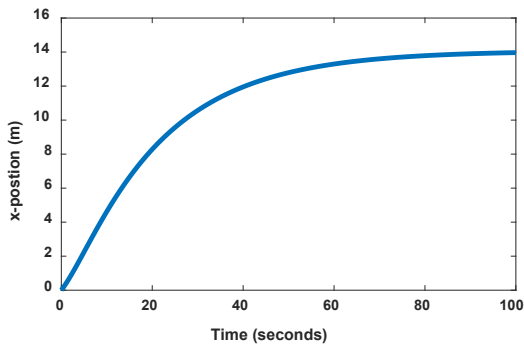


Fig. 11. Position in the  $Ox$  direction

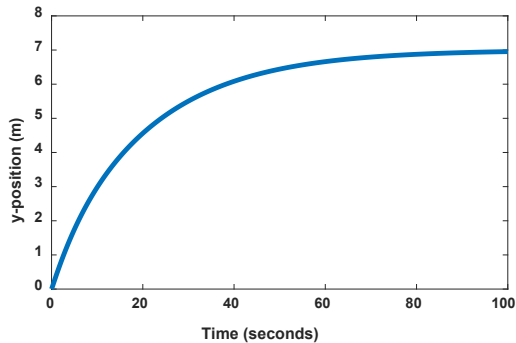


Fig. 12. Position in the  $Oy$  direction

### 3.2. Simulation Hierarchical Sliding Mode Controller

To verify the quality of the HSMC, the simulation was performed for the new S-AUV with parameters as shown in Table 2, 3.

The simulation results for S-AUV with HSMC controller are shown in Figs.11-18:

Table 2. Modeling parameter S-AUV

$m$	18.5	$Y_r$	-1.03	$N_r$	-12.32
$x_g, y_g$	0.15	$Y_v$	-0.85	$N_v$	0.32
$z_g$	0	$Y_{ v }$	-0.62	$N_{\dot{r}}$	-2.15
$X_u$	6.53	$Z_w$	4.57	$I_z$	1.57
$X_{u u }$	-0.58	$Z_{\dot{u}}$	0.23	$Y_v$	0.08

Table 3. Parameters of HSMC controller

$k$	100
$\delta$	5
$k_1$	0.05
$k_2$	5
$\lambda$	500
$\beta$	2.5
$\eta_{1d}$	$[14 \ 7]^T$
$\eta_{2d}$	$[-12 \ 0]^T$

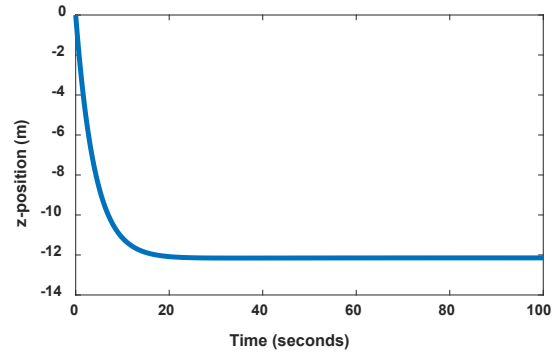


Fig. 13. Position in the  $Oz$  direction

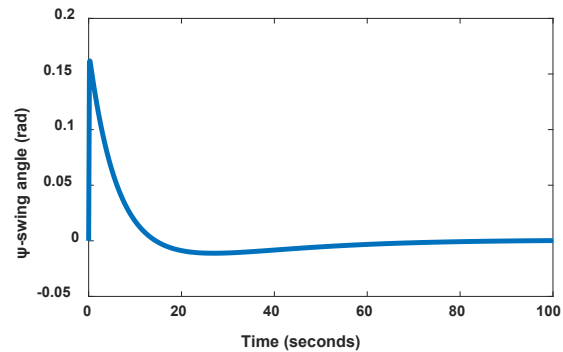


Fig. 14. Navigation angle of S-AUV

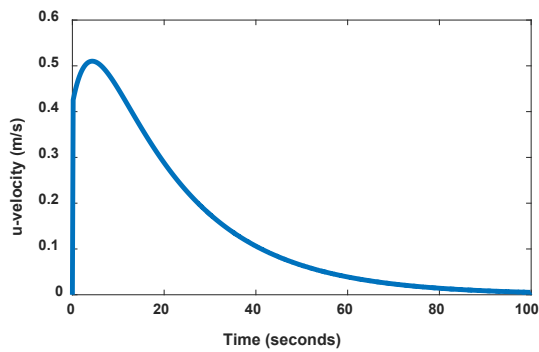


Fig. 15. Velocity in the  $Ox$  direction

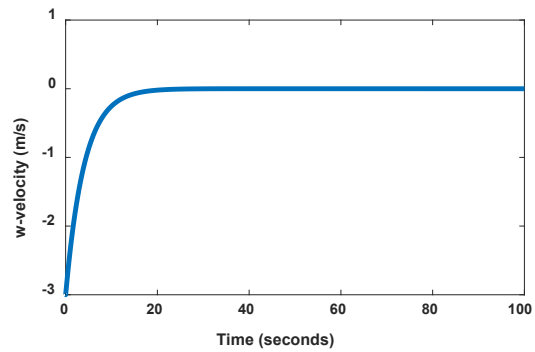


Fig. 17. Velocity in the  $Oz$  direction

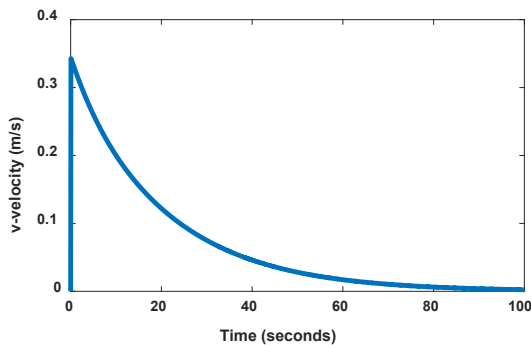


Fig. 16. Velocity in the  $Oy$  direction

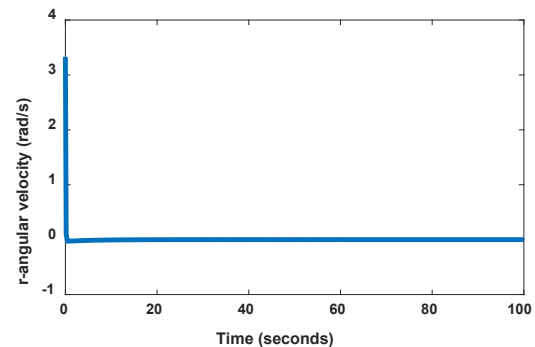


Fig. 18. Angular velocity of S-AUV navigation

According to Figs. 11-18, the HSMC applied to the new S-AUV gives good control quality in terms of grip position, directional angle, long velocity and maneuverability and angle velocity in 3-dimensional space. Specifically, the set time of the system of the grip position in the direction  $Ox$ ,  $Oy$  are respectively 84s and 86s, and the setting time of the position in the direction  $Oz$  is 20s and navigation angle is 40s.

#### 4. Conclusion

The paper presents an Autonomous Underwater Vehicles with solar energy supplemented. Applying the analysis and experimental results, when collecting solar energy, the S-AUV floats as close to the water surface as possible. Especially, when integrating retractable solar wing increases the solar collector capacity when the S-AUV's energy wing is opened to about 2.7 times compared to the closed solar wing. According to the simulation results, the HSMC controller performs control good quality. Although the setting time is rather large and the oscillation still remains when switching around the sliding surface, the simulation values approach closely to the desired setting and the overshoot is acceptable. The controller follows the desired signal with a negligible transient of less than 5%. In the future, applying the Adaptive Neural Network Controller to approximate the parameters might be a proper solution to improve the quality of control.

#### References

- [1]. U.S. Commission on Ocean Policy, An ocean blueprint for the 21st century, final report, Washington D.C., 2004, ISBN# 0-9759462-0-X.
- [2]. Denise M. Crimmins, Christopher T. Patty. Long-Endurance Test Results of the Solar-Powered AUV System, 2006, 1-4244-01 15-1/06. IEEE.
- [3]. <http://nangluongvietnam.vn/news/vn/dien-hat-nhan-nang-luong-tai-tao/cap-nhat-so-lieu-khao-sat-cuong-do-buc-xa-mat-troi-o-viet-nam.html>.
- [4]. Nguyen Van Tuan, Dinh Van Phong, Nguyen Chi Hung and Hoang The Phuong. Studying the effects of the energy wing on the motion resistance of the AUV when integrating the solar collection system. The 10<sup>th</sup> National Mechanical Conference, December 2017. ISBN 978-604-913-719-8. pp309-318.
- [5]. T. I. Fossen, O.-E. Fjellstad (1995) Nonlinear modelling of marine vehicles in 6 degrees of freedom. Mathematical Modelling of Systems, 1995, vol. 1 no. 1, pp. 17–27  
<https://doi.org/10.1080/13873959508837004>
- [6]. Wadoo S, Kachroo, Autonomous underwater vehicles: modeling, control design and simulation. CRC Press, February 2011. ISBN 978-1439818312.
- [7]. Cooney LA, Dynamic response and maneuvering strategies of a hybrid autonomous underwater vehicle in hovering. Thesis of Master of Science in ocean engineering, Massachusetts Institute of Technology, 2009.

- [8]. Buckham BJ, Podhorodeski RP, Soyly S , A chattering-free sliding-mode controller for underwater vehicles with fault tolerant infinity-norm thrust allocation. *J Ocean Eng*, 2008, 35(16):1647–1659. <https://doi.org/10.1016/j.oceaneng.2008.07.013>
- [9]. Qi X, Adaptive coordinated tracking control of multiple autonomous underwater vehicles. *Ocean Eng*, 2014, 91:84–90. <https://doi.org/10.1016/j.oceaneng.2014.08.019>
- [10]. Jun SW, Kim DW, Lee HJ, Design of T-S fuzzy model based controller for depth control of autonomous underwater vehicles with parametric uncertainties. In: 2011 11th international conference on control, automation and systems, ICCAS 2011, Gyeonggi-do, Republic of Korea, 2011, pp 1682–1684.
- [11]. Medagoda L, Williams SB, Model predictive control of an autonomous underwater vehicle in an in situ estimated water current profile. *Oceans*, 2012, Yeosu, pp 1–8. <https://doi.org/10.1109/OCEANS-yeosu.2012.6263604>
- [12]. Xu B, Pandian SR, Sakagami N, Petry F, Neurofuzzy control of underwater vehicle-manipulator systems. *J Franklin Institute*, 2012, 349(3):1125–1138. <https://doi.org/10.1016/j.jfranklin.2012.01.003>